



# Investigation on cutting edge preparation and FEM assisted optimization of the cutting edge micro shape for machining of nickel-base alloy

M. Tiffe<sup>1</sup> · R. Aßmuth<sup>1</sup> · J. Saelzer<sup>1</sup> · D. Biermann<sup>1</sup>

Received: 27 November 2018 / Accepted: 5 April 2019 / Published online: 11 April 2019  
© German Academic Society for Production Engineering (WGP) 2019

## Abstract

The productivity and the tool life of cutting tools are majorly influenced by the cutting edge micro shape. The identification of optimized cutting edges is usually based on empirical knowledge or is carried out in iterative investigation steps. This paper presents an approach to predict optimal cutting edge micro shapes with the aid of finite-element-simulations of the chip formation. The approach is investigated for the machining of the nickel-base alloy Inconel 718. The cutting edges are prepared by pressurized air wet abrasive jet machining. Utilizing this method, the prepared cutting edges have a certain profile, which is considered for the modelling. By applying a model for tool wear the influence of the cutting edge micro shape on the tool life span is estimated. Subsequently, a statistical modelling provides the prediction of the tool wear rate for any possible parameter set within the investigated range. This is used to find an optimized cutting edge profile that minimizes the tool wear. An experimental investigation concludes the optimization procedure.

**Keywords** Wet abrasive jet machining · Chip formation simulation · Cutting edge preparation · Tool wear · Optimization · Nickel-base alloy

## 1 Introduction

The cutting edge preparation is used to increase the productivity of machining processes and to enhance the wear resistance of cutting tools. The preparation primarily influences the cutting edge micro shape of the tool. The micro shape is the active part of the cutting tool where the effective rake angle differs from the nominal rake angle which is defined by the macroscopic geometry [1]. After grinding tools exhibit relatively sharp cutting edges with minor defects. Specific preparation processes are used to remove these defects, to strengthen the cutting edge and to enhance the coating adhesion by generating a rounded micro shape [2].

In order to quantify the cutting edge rounding various characterization methods were developed. Denkena et al. proposed parameters  $S_\alpha$  and  $S_\gamma$  which represent distances

between the ideal sharp cutting edge to the separation point of the cutting edge rounding at the flank face or the rake face, respectively [3]. Both values are combined to the arithmetic mean specified as  $\bar{S}$ . Further parameters of this method are the profile flattening  $S_\beta$  and the apex angle  $\varphi$  which determine the shortest distance and the shift between the ideal sharp tool tip and the cutting edge rounding. Yussefian and Koshy analyzed different prepared cutting edges and found that the cutting edge profile match well with a parabola [4]. Consequently, they proposed a parabolic description of the cutting edge micro shape. Uhlmann et al. propose another characterization method [5]. The effective rake angle and clearance angle are plotted as a function of the cutting edge profile. The lowest point of the cutting edge separates the rake face from the flank face and exhibits an effective rake angle of  $\gamma_{\text{eff}} = -90^\circ$  and an effective clearance angle of  $\alpha_{\text{eff}} = 0^\circ$ .

Investigations showed that not only the size of the cutting edge rounding but also the shape determine the process condition as well as tool related objectives [6–8]. Especially the tool life has been the objective of several investigations. Chen et al. found that the tool life is longest for drilling mold steel when the average cutting edge rounding is in the

✉ R. Aßmuth  
robert.assmuth@tu-dortmund.de

<sup>1</sup> Institute of Machining Technology, TU Dortmund University, Baroper Straße 303, 44227 Dortmund, Germany

range of  $\bar{S}=24\text{--}27\ \mu\text{m}$  [9]. A similar rounding ( $\bar{S}=30\ \mu\text{m}$ ) was identified as best by Basset et al. for orthogonal turning of AISI 1045 steel [10]. Further investigation analyzed the influence of the cutting edge segments on flank face  $S_\alpha$  and rake face  $S_\gamma$  on the tool wear for various steels. It could be shown that the flank wear mainly depends on  $S_\alpha$  while the crater wear and breakouts are influenced by  $S_\gamma$  [11, 12]. When turning AISI 1045 steel, the tool life was maximum for an asymmetrical cutting edge micro shape with  $S_\alpha=30\ \mu\text{m}$  and  $S_\gamma=60\ \mu\text{m}$  [11].

The preparation of cutting edges can be carried out via various processes. Common methods are brushing [10], dry and wet abrasive jet machining [8, 13, 14] as well as drag finishing [15]. The adjustment of the micro shape through the use of preparation processes is generally based on empirical knowledge or is carried out in iterative investigation steps. Therefore, improvements of cutting tools are obtained with high experimental efforts.

Since the finite-element-method is utilized for the simulation of chip formation it is also adopted to analyze the influence of the cutting edge micro shape on the process conditions as well as on tool and workpiece related characteristics. Denkena et al. showed a stagnation zone of the material flow in front of the cutting edge that expands with an increasing cutting edge rounding [16]. Yen et al. proved increasing mechanical loads with an increasing cutting edge rounding [17]. They further showed that the maximum tool temperature is lowest for an average cutting edge radius. This is explained by two mechanisms influencing the heat balance within the tool. On the one hand, an increasing cutting edge enhances the plastic deformation of the workpiece and thus the heat dissipation. On the other hand, the heat distribution is more homogeneous for a bigger rounding leading to a decrease of the maximum temperature. One major objective of the FE-simulation is the tool wear that is often simulated with respect to the Usui-equation [18]. Yen et al. modelled the progression of the tool wear in a two-dimensional simulation by updating the tool geometry [19]. Klocke and Frank [20] as well as Attanasio et al. [21] used an extension of this approach for three-dimensional simulations of hard turning.

## 2 Optimization approach

In order to optimize the cutting edge micro shape of a tool, a specific experimental design, which combines FE-simulation and statistical modelling, is used (see Fig. 1). First, a parametric description of the cutting edge in terms of the established form factor method is adopted to utilize an experimental design for a variation of the cutting edge. In this respect, the parameters  $S_\alpha$ ,  $S_\gamma$ ,  $S_\beta$  and  $\varphi$  determine the cutting edge. Besides these parameters, process parameters like the

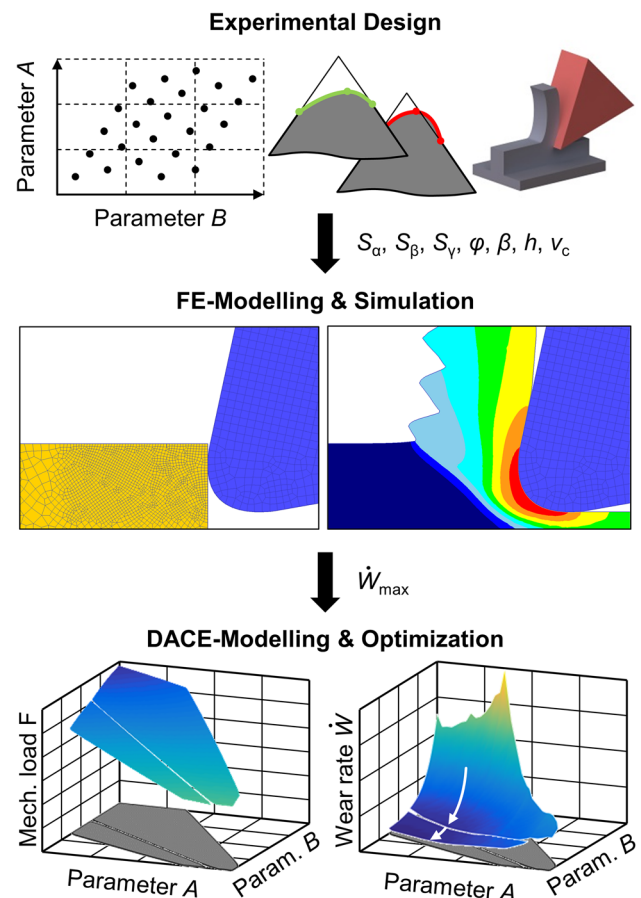


Fig. 1 Approach for the optimization of the cutting edge micro shape

cutting speed  $v_c$  and the uncut chip thickness  $h$  as well as the wedge angle  $\beta$  can be included, too. Certain parameter combinations are used to set up FE-models for chip formation simulation. Within the simulations the tool wear rate is calculated by means of the wear model proposed by Usui [18]:

$$\dot{W} = a\sigma_n v_s e^{-\frac{b}{T_{\text{tool}}}}$$

Here,  $\sigma_n$  is the contact normal pressure,  $v_s$  is the sliding velocity and  $T_{\text{tool}}$  is the tool temperature. The model parameters are set to  $a=3.6e^{-9}$  and  $b=1200$  for Inconel 625 according to Lotfi [22]. The wear rate is calculated for all contact nodes of the tool. The maximum wear rate of each simulation  $\dot{W}_{\text{max}}$  is used as the optimization criterion and acts as the objective for a statistical modelling of the cutting edge influence on the wear rate. So called DACE-models (design and analysis of computer experiments) are calculated to predict the wear rate for any cutting edge within the investigated range [23]. These models are further used to find cutting edges that minimize the tool wear for specified process parameters.

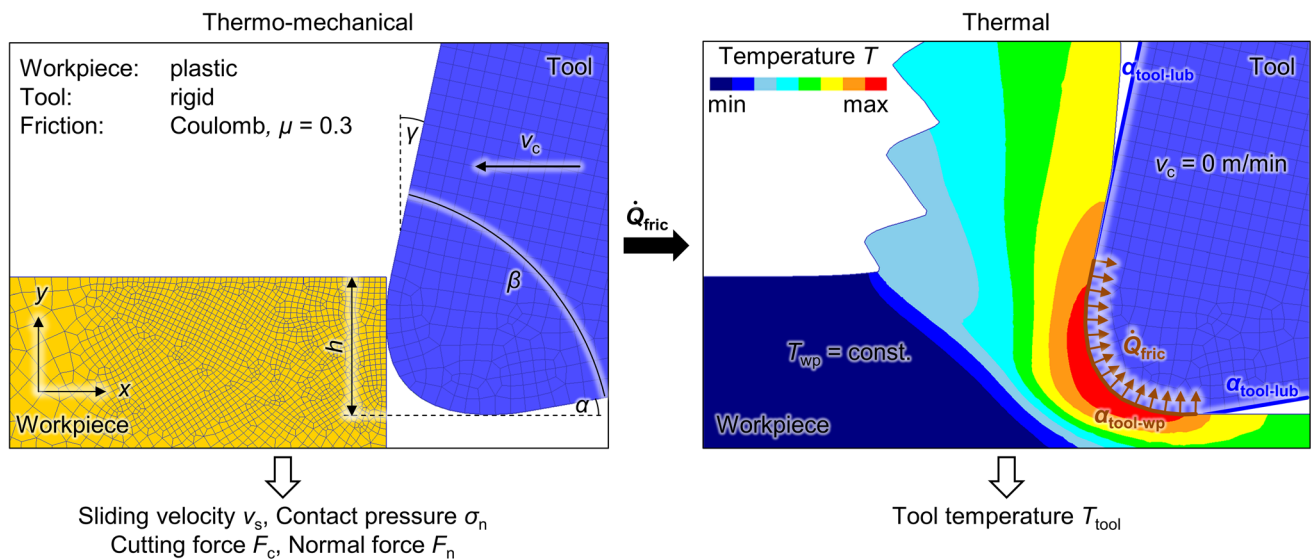


Fig. 2 Modeling of the chip formation under plane strain conditions

### 3 Modelling and simulation

#### 3.1 FE-modeling and validation

For the analysis of the tool load or the wear behavior of prepared cutting edges, respectively, the FE-software DEFORM 2D is used. It provides an implemented remeshing routine to renew the finite element mesh and to maintain the solvability of the FE-problem throughout the simulation. Therefore, the software is capable to capture large strains those occur during chip formation processes. In this context, the 2D simulation enables a sufficiently high resolution of the material flow in the area of the cutting edge as well as the general analysis of the influence of the cutting edge rounding on the chip formation. This ensures that the results are largely transferable to different machining processes. A two-step model is setup under plane strain conditions which is shown in Fig. 2. First, a fully thermo-mechanical coupled model is used to simulate the chip formation. The material behavior of the workpiece is assumed to be pure plastic with an isotropic hardening. In order to calculate flow stresses at high strain rates and temperatures the Johnson–Cook-flow stress model is used with parameters provided by Klocke et al. [24]. Furthermore, the normalized Cockroft–Latham-model is applied to obtain the typical segmentation of the chips [24]. The tool with a wedge angle of  $\beta$  is perfectly rigid and can transfer heat. An interaction between the tool and the workpiece is considered by applying Coulomb’s law with a friction factor of  $\mu = 0.3$ . The workpiece is positioned and fixed in the  $x$ – $y$ -space in the way that an uncut chip thickness of  $h$  is achieved and a clearance angle of  $\alpha$  or a rake angle of  $\gamma$ , respectively, is obtained. The cutting

motion is carried out by the tool with a cutting speed of  $v_c$  in negative  $x$ -direction. The process of chip formation is simulated until a steady state chip formation is reached. Finally, the sliding velocity and the contact pressure can be extracted.

The simulated process time of the first step lies in the range of a few microseconds, which is long enough to achieve a constant mechanical tool load. Nevertheless, the tool temperature strongly depends on the thermal loading history of the process and a longer process time has to be simulated to reach a steady state. Therefore, a subsequent model is used to exclusively calculate the heat transfer within the tool over an interval of several seconds. In this simulation no cutting motion is active ( $v_c = 0$  m/min). The frictional heat  $\dot{Q}_{fric}$  for each contact node is derived from the thermo-mechanical simulation and is applied as stationary heat source on the tool. In addition, the temperature in the workpiece  $T_{wp}$  remains constant which leads to a heat flow from the workpiece to the tool due to the heat transfer coefficient of  $\alpha_{tool-wp} = 40$  kW/m<sup>2</sup> K. The cooling by the lubrication fluid is set to  $\alpha_{tool-lub} = 20$  kW/m<sup>2</sup> K in the area where no tool-workpiece contact is present. The simulation model was validated by means of chip formation comparison, force and temperature measurements [25].

#### 3.2 Modelling of honed/prepared cutting edges and experimental design

In order to optimize the cutting edge micro shape it is necessary to characterize the edge profile by a parametric description. Therefore, the influence of the micro shape can be analyzed through a variation of the parameters in a certain experimental design. In this regard, the parameters  $S_\alpha, S_\gamma, S_\beta$

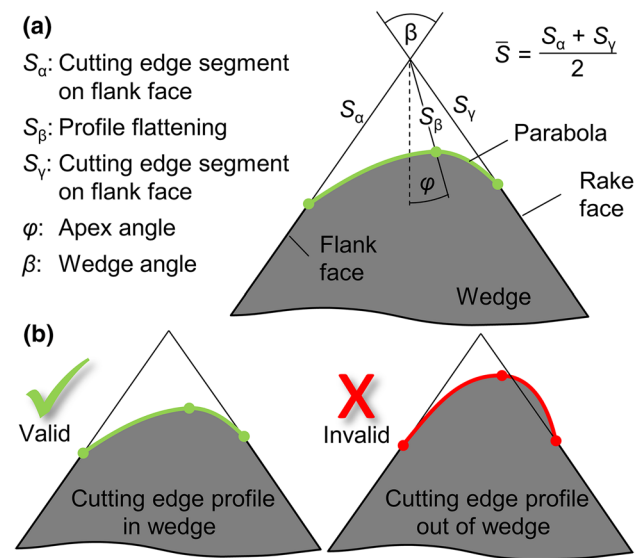


**Fig. 3** **a** Modelling of honed/prepared cutting edge with a parabolic shape. **b** Distinction between valid and invalid cutting edge profiles

and  $\varphi$  are used as proposed by Denkena et al. [3]. The average cutting edge rounding can be considered by the value of  $\bar{S}$ . Although, this description of cutting edges has gained popularity in the scientific community over the last decade, the sole use of these parameters is not sufficient to model cutting edge profiles for the purpose of FE-simulation. The parameters determine three points on the cutting wedge but the connecting cutting edge profile between them remains unknown. Yusefian and Koshy analyzed the micro shape of rounded cutting edges and found a good approximation by using a parabolic contour [4]. These two approaches can be combined to achieve a parametric description of the cutting edge as it is shown in Fig. 3a. It can be seen, that the cutting wedge is determined by the four cutting edge parameters as well as the wedge angle. When modelling the cutting edge certain parameter sets lead to profiles that exceed the wedge boundaries (Fig. 3b). Such profiles cannot be achieved by conventional preparation methods. As a consequence a distinction between valid and invalid cutting edge profiles is made. Only convex profiles that are located within the wedge are considered for the wear analysis.

With respect to the experimental validation of the simulation findings pressurized air wet abrasive jet machining (PAWAJM) is utilized to prepare the cutting edge. The influence of various process parameters on the cutting edge micro shape was analyzed in extensive investigations. Among other things, the influence of the jet pressure, the jet feed speed, the jet inclination angle and the jet nozzle distance on the size and shape of the cutting edge rounding was investigated. The results showed a correlation between the average cutting edge rounding  $\bar{S}$  and the profile flattening  $S_\beta$ . In order to describe this correlation, a new characterization parameter

#### Pressurized air wet abrasive jet machining

Jet medium:	Water, ZWSK F220
Jet pressure:	$p_{st} = 6$ bar
Jet feed speed:	$v_{f,st} = 0 \dots 8$ mm/s
Jet nozzle distance:	$h_d = 20$ mm
Jet inclination angle:	$\alpha_{st} = 0^\circ$
Abrasive vol. concn.:	$\sigma_{st} = 12\%$
Workpiece:	Cemented carbide rods
Wedge angle:	$\beta = 45 \dots 80^\circ$

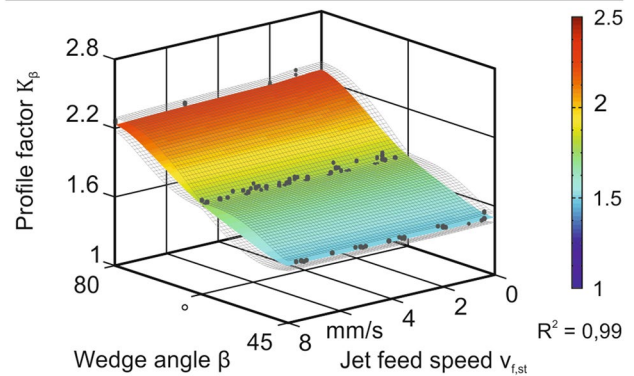


**Fig. 4** Profile factor: profile factor for PAWAJM

is introduced. The profile factor  $K_\beta$  represents the ratio of  $\bar{S}$  to  $S_\beta$ :

$$K_\beta = \frac{\bar{S}}{S_\beta}$$

The profile factor provides information about the shape of the cutting edge in relation to the profile contour between rake and flank face. The higher the level of  $K_\beta$ , the more pointed is the profile. Conversely, the profile is flatter at lower  $K_\beta$  levels. With respect to the PAWAJM no significant influence of the process parameters on the  $K_\beta$  was identified when preparing cemented carbide cutting edges. In contrast, the value of  $K_\beta$  strongly depends on the wedge angle  $\beta$  (Fig. 4). This means that, regardless of the specific process control in PAWAJM, a similar ratio of  $\bar{S}$  to  $S_\beta$  is generated and the cutting edges have comparable curvatures for identical wedge angles.

Consequently, the value of  $K_\beta$  can be approximated as a function of  $\beta$ :

$$K_\beta(\beta) = 0.939e^{(0.0106\beta)}$$

For the analysis of the influence of the cutting edge micro shape on the wear of a drilling tool a certain experimental design is used for a subsequent empirical modelling. A Latin hypercube design is utilized to vary the parameters on a high amount of levels while keeping the number of simulations low. The intervals for the cutting edge parameters are chosen as follows:  $S_\alpha = 20\text{--}100$   $\mu\text{m}$ ,  $S_\gamma = 20\text{--}100$   $\mu\text{m}$  and



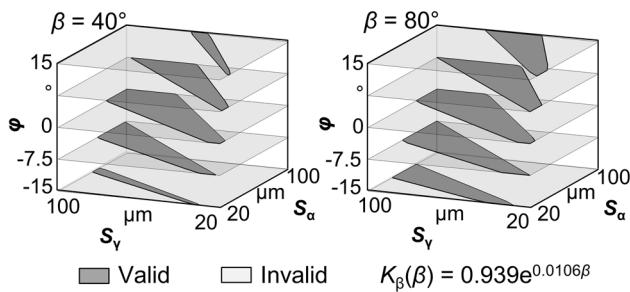


**Fig. 5** Graphical representation of valid and invalid parameter sets of cutting edge roundings for wedge angles of  $\beta=40^\circ$  and  $\beta=80^\circ$

$\varphi = -15^\circ$  to  $15^\circ$ . A distinction between valid and invalid cutting edges is made and has to be taken into account for the experimental design. Furthermore, the findings from the PAWAJM investigations are used for the modelling of the cutting edge micro shape. In this context,  $K_\beta(\beta)$  is considered. This leads to a subdivision of the design space, which is presented in Fig. 5. It can be seen that an apex angle of  $\varphi=0^\circ$  provides a symmetric domain of valid parameter sets in the  $S_\alpha$ - $S_\gamma$ -plane. The domain is shifted towards low values of  $S_\alpha$  when  $\varphi$  decreases. In contrast, the domain exhibits low values of  $S_\gamma$  when  $\varphi$  is increased. The validity of the cutting edges does not only depend on the cutting edge parameters but also on the wedge angle. Especially when  $\varphi$  is high or low the domain of valid edges is bigger for higher wedge angles. Besides the cutting edge parameters the wedge angle as well as the process parameters  $h$  and  $v_c$  are integrated in the experimental design. Therefore, varying local process conditions, e.g., for drilling processes, can be considered, too.

The output of each simulation is used for the statistical modeling and optimization. In this particular investigation so called DACE-models are calculated to find functional relationships between the cutting edge parameters and the thermo-mechanical tool load as well as the wear rate [23].

### 4 Simulation results

The response surfaces of DACE-models for the cutting force  $F_c$  and the normal force  $F_n$  are illustrated in Fig. 6 as a function of the cutting edge segment on the flank face  $S_\alpha$  and on the rake face  $S_\gamma$  with respect to the validity of the cutting edge. The cutting force  $F_c$  increases with rising  $S_\alpha$  and  $S_\gamma$  due to an increased amount of effective negative rake angles. Low rake angles promote the compression of the workpiece material in front of the cutting edge, which leads to a higher tool load. An apex angle of  $\varphi=0^\circ$  results in a symmetrical dependency of  $F_c$  on the cutting edge segments. In contrast, the domain of valid cutting edges is asymmetric and smaller when the apex is shifted towards the flank face which is

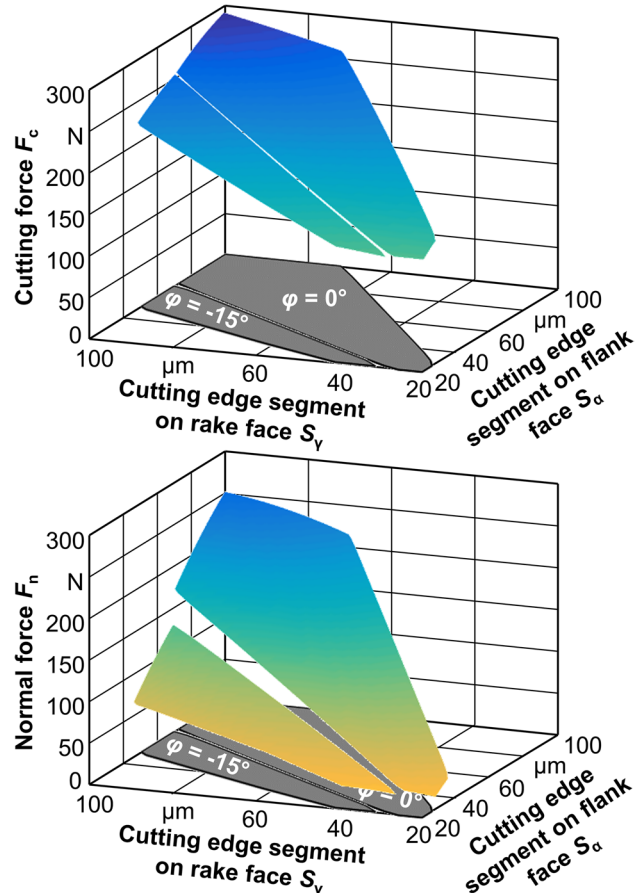
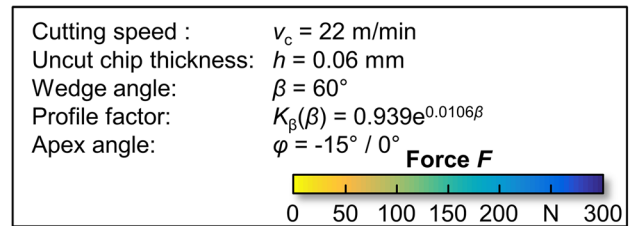


**Fig. 6** Mechanical tool loads as a function of cutting edge segments  $S_\alpha$  and  $S_\gamma$

presented for an apex angle of  $\varphi = -15^\circ$ . It can be seen that the cutting force is decreased for negative apex angles, too. This can be explained by a reduction of material compression. The displayed normal force  $F_n$  reveals a similar behavior regarding the influence of the cutting edge segments on the flank face  $S_\alpha$  and on the rake face  $S_\gamma$ . It further shows that the influence of the apex angle is even bigger on the normal force than on the cutting force. This can be traced back to the influence of the effective rake angles on the local normal forces acting on the cutting edge. An increase of the rake angle leads to a reduction of the normal force.

The response surfaces of the DACE-model for the wear rate  $W$  is illustrated in Fig. 7. It can be seen that the wear rate is majorly influenced by the cutting edge segment on

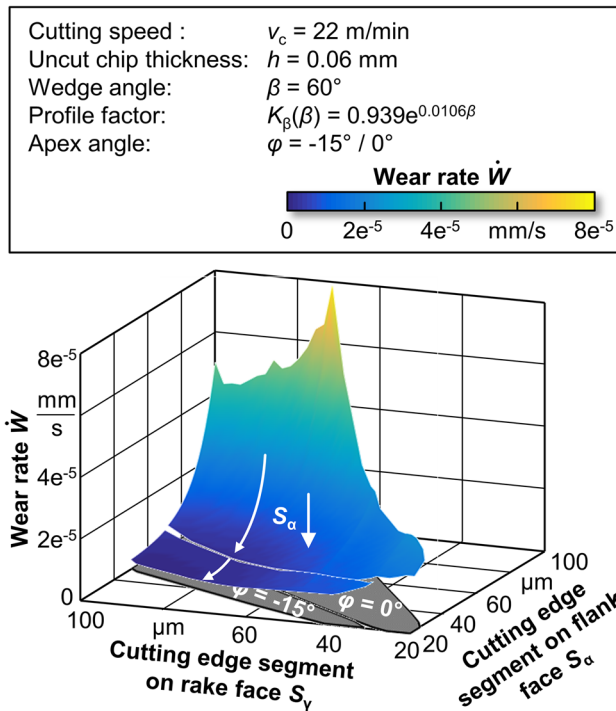


Fig. 7 Simulated maximum wear rate as a function of cutting edge segments  $S_\alpha$  and  $S_\gamma$

domain. The cutting edge segment on the rake face shows only little influence on the wear rate. A further analysis indicates that the apex angle has just a small influence on the DACE-model, too. However, since the apex angle determines the validity of cutting edges and a drop of  $\varphi$  shifts the valid domain towards low values of  $S_\alpha$ , it can influence the wear behavior of the cutting edge. As it is shown in Fig. 7 a lower wear rate can be achieved through smaller cutting edge segments on the flank face  $S_\alpha$  which is linked to a change of the apex angle from  $\varphi = 0^\circ$  to  $\varphi = -15^\circ$ .

The sliding velocity, the contact pressure and the tool temperature are used for the wear rate calculation as proposed by Usui [18]. In order to identify the cause of the reduced wear rate of the asymmetric cutting edge these parameters are analyzed. Since the contact pressure is homogeneously distributed and identical for the investigated cutting edges the sliding velocity and the tool temperature are focused at this point. In Fig. 8 the flow of the workpiece material and the tool temperature are illustrated for a nearly symmetrical and an asymmetrical cutting edge rounding. In front of the cutting edge rounding a zone of relatively slow material flow occurs. This stagnation zone was also observed by Denkena et al. [15]. On a certain point A on the cutting edge the material flow is divided into two directions. One part flows along the rake face into the chip, the other part

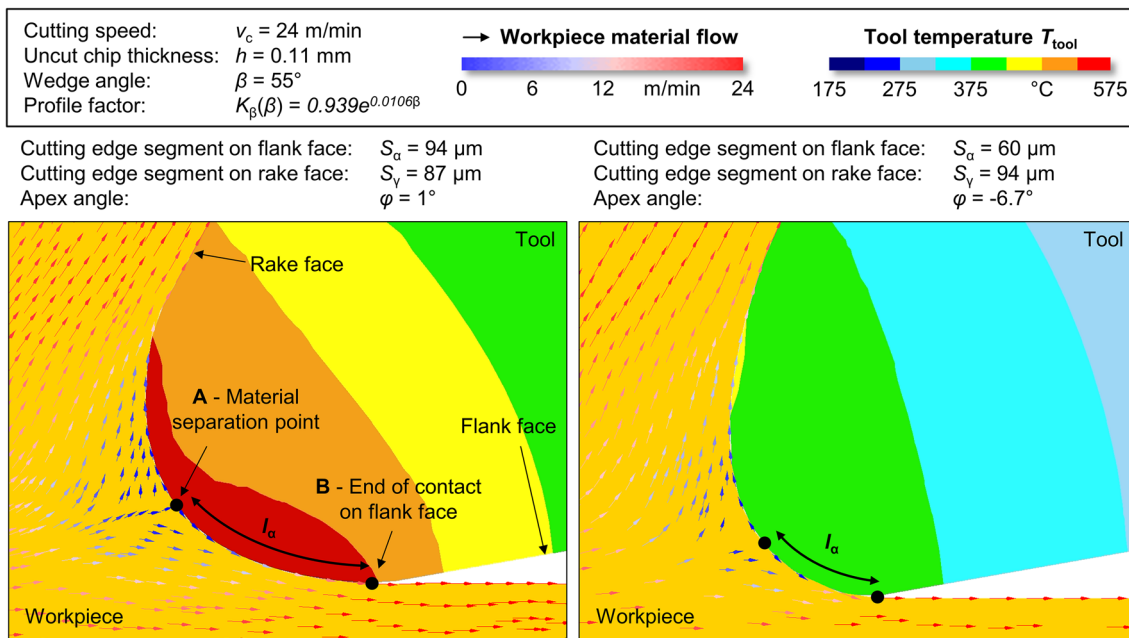


Fig. 8 Material flow and tool temperature for a nearly symmetrical and an asymmetrical cutting edge roundings

the flank face  $S_\alpha$ . The model reveals a reduction of the wear rate when  $S_\alpha$  decreases. The wear rate is the lowest when  $S_\alpha$  is chosen to be as small as possible within the valid range. Therefore, the optimum lies on the constraint of the valid

flows beneath the cutting edge to the flank face and forms the new workpiece surface. The material flow at the separation point is zero and increases along the contact length on the

flank face  $l_\alpha$  until it matches the cutting speed  $v_c$  at point B where the tool to workpiece contact ends. On the rake face the material flow increases to a level that is lower than the cutting speed due to the chip compression. These processes with the same minimum and maximum velocities can be observed for all cutting edges. In contrast, the tool temperature is different for the two presented cutting edges. The temperature of the nearly symmetrical tool is up to 575 °C while the temperature of the asymmetrical cutting edge is up to 425 °C. The tool temperature is significantly influenced by the frictional heat as well as the heat transfer from the chip and the workpiece to the tool. The amount of the induced heat for both processes is depended on the contact length between the tool and the workpiece. As it is shown in Fig. 8 the contact length on the flank face  $l_\alpha$  is decreased when the apex of the cutting edge is shifted towards the flank face. The contact on the rake face is barely influenced by the micro shape of the cutting edge. Consequently, less heat is transferred into the tool when using proper designed asymmetrical than for symmetrical cutting edges.

Finally, it can be concluded that a reduction of tool wear is mainly achieved by a reduction of the tool temperature. Therefore, the contact length on the flank face  $l_\alpha$  has to be low by choosing short cutting edge segments on the flank face  $S_\alpha$ . Since wet abrasive jet machining of cutting edges is restricted to certain combinations of the cutting edge parameters it is further necessary to shift the apex of the cutting edge towards the flank face. This finding is confirmed in 195 simulations in which the influence of the cutting parameters, the wedge angle and the micro shape of the cutting edge were investigated.

### 5 Experimental investigation

The findings of Sect. 4 are validated in a drilling process with two fluted twist drills with a diameter of  $d_{\text{tool}}=8.5$  mm made of micro-grain cemented carbide with 10% of cobalt. In order to adjust the cutting edge micro shape pressurized air wet abrasive jet machining is utilized. Due to the simulation results the following parameters are chosen as the optimized cutting edge with asymmetrical shape:  $S_\alpha=45$   $\mu\text{m}$ ,  $S_\gamma=83$   $\mu\text{m}$ ,  $S_\beta=37$  and  $\varphi=-15^\circ$ . Besides this shape an asymmetrical cutting edge with a smaller rounding ( $\bar{S}=30\pm 3$   $\mu\text{m}$ ) and a symmetrical cutting edge with an average rounding of  $\bar{S}=64\pm 5$   $\mu\text{m}$  were prepared and investigated. These three cutting edge roundings are referred as “big, asymmetric”, “small, asymmetric” and “big, symmetric”, respectively. The target preparation and the actual obtained roundings are illustrated in Fig. 9 with respect to  $S_\alpha$  and  $S_\gamma$ . The SEM-pictures give a qualitative view of the size of the rounding. It can also be seen that grinding marks are visible on the flank face of both asymmetric micro shapes

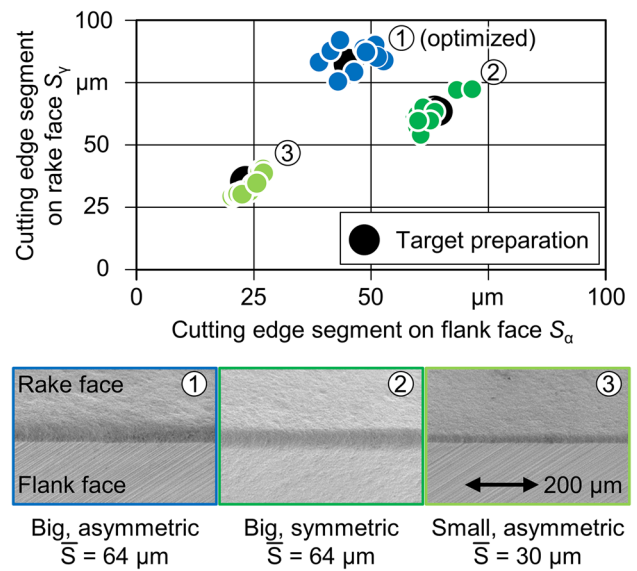


Fig. 9 Parameters and SEM-picture of prepared cutting edges of drilling tools

while the rake face and the cutting edge exhibit a dimple structure. This is the result of the abrasive jet that is primarily directed towards the rake face in order to obtain a longer cutting edge segment on the rake face than on the flank face. In contrast, the symmetric cutting edge exclusively reveals dimple structures due to an identical orientation of both faces to the abrasive jet. After the cutting edge preparation the tools have been coated with an Arc-PVD-Coating of TiAlN.

The prepared tools are used for the drilling of Inconel 718 with a cutting speed of  $v_c=30$  m/min and a feed of  $f=0.144$  mm on the machining center Grob BZ40CS. The chosen feed path is  $l_f=1.82$  m and an emulsion is used for lubrication and cooling of the tool. Since the thermomechanical load is dominant near the cutting edge corner the wear is analyzed in this area of the major cutting edge. Before and after the use of the tools the cutting edges are digitalized with the measuring microscope Alicona Infinite Focus G5. Both measurements are then positioned and aligned to quantify the differences of the edge profiles. Hence, the removed coating and substrate can be expressed as the wear volume  $V_{\text{wear}}$ . The obtained results for the three different cutting edge types of drilling tools are illustrated in Fig. 10. The error bars represent the range of the measured wear volume of four experiments per cutting edge type. Consequently, six two-fluted twist drills with a total of twelve cutting edges were investigated to validate the simulation findings. It can be seen that the wear volume is lowest for the optimized cutting edge followed by the symmetrical and the asymmetrical cutting edge with a small rounding. The difference models

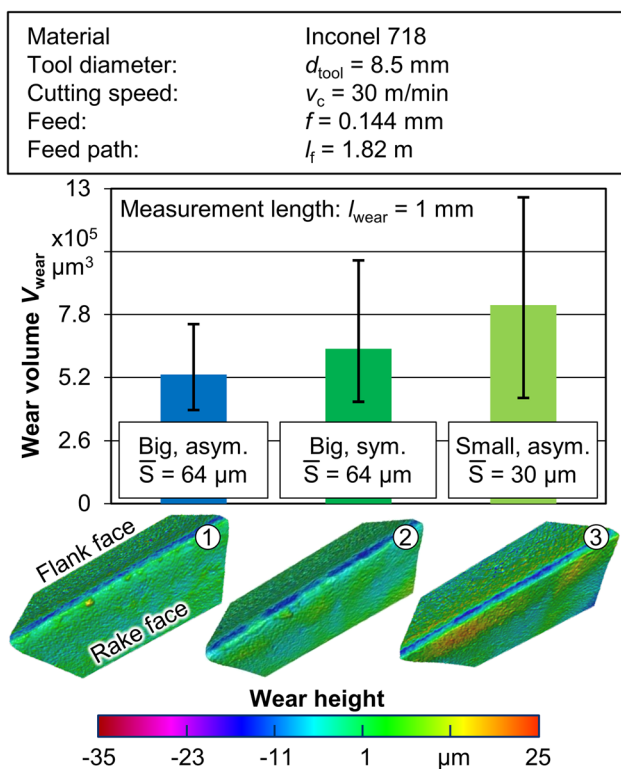


Fig. 10 Wear of drilling tools

of the displayed surfaces also show reduced wear heights of the optimized tool compared to the others.

## 6 Conclusion and outlook

This paper deals with the optimization of prepared cutting edge micro shapes. The wear rate after Usui is calculated from chip formation simulations. It serves as an optimization criterion and is analyzed by means of a particular experimental design. For the experimental design only valid cutting edge micro shapes are considered. In this context, the ratio of the average cutting edge rounding  $\bar{S}$  to the profile flattening  $S_p$  is introduced as the profile factor  $K_p$ . With respect to the pressurized air wet abrasive jet machining  $K_p$  can be described by a function of the wedge angle  $\beta$ . The mechanical tool load is dependent on the cutting edge segments  $S_\alpha$  and  $S_\gamma$  and can be reduced by shifting the apex towards the flank face ( $\varphi < 0^\circ$ ). Similar results are obtained for the wear rate. This is due to the decreased tool temperature when the contact on the flank face  $l_\alpha$  is reduced. Therefore, cutting edges with an asymmetrical micro shape are desired for the machining of Inconel 718 which is validated by drilling experiments with targeted prepared cutting edge roundings. Further investigations should consider the influence of tool coating on tool wear,

for example with regard to differences in coating adhesion or coating defects due to different cutting edge geometries.

**Acknowledgements** This paper is based on investigations of the projects “Development of a simulation based method for a load dependent optimization of cemented carbide tools for nickel-base alloys—Variable micro geometry along the cutting edge/Knowledge Transfer Project” (BI 498/75)—project number 313918187 and “Analysis of a simulation approach to model the material removal when preparing cutting edge with wet abrasive jet machining” (BI 498/89)—project number 374073886 which are kindly supported by the German Research Foundation (DFG).

## References

- Denkena B, Biermann D (2014) Cutting edge geometries. CIRP Ann Manuf Technol 63:631–653
- Bouzakis K-D, Michailidis N, Skordaris G, Bouzakis E, Biermann D, M’Saoubi R (2012) Cutting with coated tools: coating technologies, characterization methods and performance optimization. CIRP Ann Manuf Technol 61(2):703–723
- Denkena B, Friemuth T, Fedorenko S, Groppe M (2002) An der Schneide wird das Geld verdient—Neue Parameter zur Charakterisierung der Schneidengeometrien an Zerspanwerkzeugen. Werkzeuge—Sonderausgabe der Zeitschrift Fertigung 30(2):24–26
- Yuseffian NZ, Koshy P (2013) Parametric characterization of the geometry of honed cutting edges. Precis Eng 37:746–752
- Uhlmann E, König J, Dethlefs A, Graf v. d. Schulenburg M (2011) Charakterisierung geometrisch bestimmter Schneiden. Wt Werkstattstechnikonline 101(7/8):475–481
- Biermann D, Baschin A (2009) Influence of cutting edge geometry and cutting edge radius on the stability of micromilling processes. Prod Eng Res Dev 3(4–5):375–380
- Denkena B, Lucas A, Bassett E (2011) Effects of the cutting edge microgeometry on tool wear and its thermo mechanical load. CIRP Ann Manuf Technol 60(1):73–76
- Wyen C-F (2011) Rounded cutting edges and their influence in machining titanium. Dissertation, ETH Zürich, Zürich
- Cheung FY, Zhou ZF, Geddam A, Li KY (2008) Cutting edge preparation using magnetic polishing and its influence on the performance of high-speed steel drills. J Mater Process Technol 208:196–204
- Bassett E, Köhler J, Denkena B (2012) On the honed cutting edge and its side effects during orthogonal turning operations of AISI1045 with coated WCCo inserts. CIRP J Manuf Sci Technol 5:108–126
- Bassett E (2014) Belastungsspezifische Auslegung und Herstellung von Schneidkanten für Drehwerkzeuge. Dissertation, Leibniz Universität Hannover
- Bergmann B (2017) Grundlagen zur Auslegung von Schneidkantenverrundungen. Dissertation, Leibniz Universität Hannover
- Cortes Rodriguez CJ (2009) Cutting edge preparation of precision cutting tools by applying micro-abrasive jet machining and brushing. Dissertation, Universität Kassel
- Terwey I (2011) Steigerung der Leistungsfähigkeit von Vollhartmetallwendelbohrern durch Strahlspanen. Technische Universität Dortmund
- Risse K (2006) Einflüsse von Werkzeugdurchmesser und Schneidkantenverrundung beim Bohren mit Wendelbohrern in Stahl. Dissertation RWTH Aachen



16. Denkena B, Köhler J (2012) Mesfin Sisay Mengesha: influence of the cutting edge rounding on the chip formation process: Part 1. Investigation of material flow, process forces, and cutting temperature. *Prod Eng* 6(4–5):329–338
17. Yen Y-C, Jain A, Altan T (2004) A finite element analysis of orthogonal machining using different tool edge geometries. *J Mater Process Technol* 146(1):72–81
18. Usui E, Shirakashi T, Kitagawa T (1984) Analytical prediction of cutting tool wear. *Wear* 100:129–151
19. Yen Y-C, Söhner J, Lilly B, Altan T (2004) Estimation of tool wear in orthogonal cutting using the finite element analysis. *J Mater Process Technol* 146(1):82–91
20. Klocke F, Frank P (2009) Verschleißsimulation von cBN-Schneidplatten beim Hartdrehen. *Wt Werkstattstechnikonline* 99(1/2):35–41
21. Attanasio A, Ceretti E, Giardini C 3D FEM simulation of flank wear in turning. In: *Proceedings of the 14th international Esaform conference on material forming*, pp 561–566
22. Lotfi M, Jahanbakhsh M, Akhavan Farid A (2016) Wear estimation of ceramic and coated carbide tools in turning of Inconel 625: 3D FE analysis. *Tribol Int* 99:107–116
23. Sacks J, Welch WJ, Mitchell TJ, Wynn HP (1989) Design and analysis of computer experiments. *Stat Sci* 4:409–435
24. Klocke F, Lung D, Buchkremer S (2013) Inverse identification of the constitutive equation of inconel 718 and AISI 1045 from FE machining simulations. *Proc CIRP* 8:212–217
25. Biermann D, Abmuth R, Hess S, Tiffe M (2018) Simulation based analysis and optimisation of the cutting edge micro shape for machining of nickel-base alloys. *Proc CIRP* 67:284–289

**Publisher's Note** Springer Nature remains neutral with regard to jurisdictional claims in published maps and institutional affiliations.